*Original Article*

DOI: 10.5582/ddt.2025.01105

# Comparative study of contrast-enhanced ultrasound and contrast-enhanced computed tomography in the diagnosis of benign and malignant lesions of the gallbladder

**Liang Fang[1,§], Zhiying Qiu[1,§], Lingwen Xu[1], Fei Hu[2], Yuchen Tao[1], Shengnan Ding[1], Jing Zhou[3], Ling Wang[4,*], Lin Chen[1,*]**

[1] Department of Ultrasonic Diagnosis, Huadong Hospital Affiliated to Fudan University, Shanghai, China;
[2] Department of radiology, Huadong Hospital Affiliated to Fudan University, Shanghai, China;
[3] Department of Obstetrics and Gynecology, Nanfang Hospital, Southern Medical University, Guangzhou, Guangdong, China;
[4] Department of Obstetrics, The First Affiliated Hospital, Guizhou University of Traditional Chinese Medicine, Guiyang, China.

**SUMMARY**: This study compared the diagnostic value of contrast-enhanced ultrasound (CEUS) and contrast-enhanced computed tomography (CECT) for differentiating benign and malignant gallbladder (GB) lesions. A retrospective analysis was performed on 151 hospitalized patients with GB lesions: 74 underwent CEUS alone, 25 CECT alone, and 52 both examinations preoperatively. Histopathology served as the reference standard. Imaging features of benign/malignant lesions were compared using *t*-test or chi-square ($\chi^2$) test; CEUS quantitative parameters were analyzed *via t*-test. Diagnostic efficacy of the two modalities was compared by $\chi^2$ test. Of 151 patients, 57 (37.7%) had malignant and 94 (62.3%) benign lesions. Statistically significant differences between benign and malignant groups were observed in CEUS/CECT features (vascular enhancement morphology, contrast distribution, GB wall integrity, ill-defined borders with adjacent liver) and CEUS washout time (WT) (all $P < 0.05$). In the entire cohort, no significant differences existed between CEUS and CECT in sensitivity (89.2% *vs.* 85.7%), specificity (78.8% *vs.* 74.3%), accuracy (84.9% *vs.* 80.5%), positive predictive value (PPV) (85.7% *vs.* 80.0%) and negative predictive value (NPV) (83.7% *vs.* 81.2%) (all $P > 0.05$). Similar non-significant differences were noted in the 52-patient subgroup (sensitivity: 65.0% *vs.* 80.0%; specificity: 62.5% *vs.* 80.0%; accuracy: 63.5% *vs.* 76.9%; PPV: 40.6% *vs.* 50.0%; NPV: 51.3% *vs.* 66.7%; all $P > 0.05$). CEUS is effective for differentiating benign and malignant GB lesions, with diagnostic efficacy comparable to CECT.

***Keywords***: contrast enhanced ultrasound (CEUS), gallbladder cancer (GBC), contrast enhanced CT (CECT)

## 1. Introduction

Gallbladder cancer (GBC) can originate from multiple sites such as the fundus, body, neck of the gallbladder (GB), or cystic duct, accounting for approximately 80% to 95% of biliary tract malignancies (*1,2*), making it the most common biliary tract malignancy. Due to its insidious onset and highly aggressive nature, most GBC patients are diagnosed at advanced stages, with a 5-year survival rate < 20% in most countries (*3-9*). Therefore, improving the diagnoses and early detection rate of GBC is crucial for the treatment of GBC and has significant implications for enhancing the survival rate of GBC patients.

Contrast-enhanced computed tomography (CECT) enables hepatobiliary scanning during arterial or portal phase within a single breath-hold and allows thin-section (1 mm) scanning of the region of interest, significantly increasing the lesion detection rates. However, CECT has its limitations. Firstly, as a timed scanning technique, it cannot achieve prolonged continuous scanning, potentially missing lesion enhancement at specific time points. Secondly, restricted by planar imaging, it only provides transverse cross-section views. Thirdly, CECT is contraindicated for patients with allergy to the iodine contrast agent, renal insufficiency, or severe hyperthyroidism. Finally, CECT is costly and involves radiation exposure. Thus, exploring for an imaging diagnostic modality that complements CECT is particularly crucial for clinical practice.

Given the excellent contrast between bile within GB and the GB wall, intramural lesions, stones, and adjacent liver tissue, coupled with its superior spatial resolution compared to other tomographic methods, conventional

ultrasound (US) has become a common imaging method for detecting and diagnosing GB lesions (*10,11*). However, conventional US has limitations in visualizing GB wall integrity at the lesion and lesion vascularity (*12*).

Contrast-enhanced ultrasound (CEUS), a technically simple imaging modality utilizing microbubble contrast agents and contrast-specific US modes, has been introduced to overcome the limitations of B-mode and color Doppler US. CEUS has been increasingly used in abdominal diseases, with diagnostic efficacy comparable to CECT and contrast-enhanced magnetic resonance imaging (CEMRI) (*13,14*). Several studies have explored the role of CEUS in GB malignancies (*11,15-18*). However, comparative studies between CEUS and CECT for differentiating benign and malignant GB diseases remain scarce. The objective of this study was to investigate the sensitivity and specificity of CEUS and CECT in GBC by comparing pathological findings.

## 2. Methods

### 2.1. Patients

A retrospective analysis was conducted on 151 patients with GB diseases who were admitted to Huadong Hospital Affiliated to Fudan University and underwent surgical treatment between January 2020 and June 2025. All patients had confirmed pathological results. Before surgery, the patients underwent either CEUS, CECT, or both examinations: 126 patients underwent CEUS (CEUS group), which included 74 patients who underwent CEUS alone and 52 patients who underwent both CEUS and CECT; 77 patients underwent CECT (CECT group), which included 25 patients who underwent CECT alone and 52 patients who underwent both examinations. 126 patients (51males and 75 females; age range 29 to 90 years with an average of 64.6 ± 9.3 years; lesion diameter 11 to 136 mm with an average of 43.5 ± 27.4 mm) were examined by CEUS (CEUS group), 77 (32 males and 45 females; age range 37 to 81 years with an average of 63.2 ± 10.9 years; lesion diameter 14 to 58 mm with an average of 31.6 ± 17.2 mm) were examined by CECT (CECT group). In the two groups, 52 patients (21 male and 31 female; age range 32 to 87 years with an average of 63.1 ± 10.3 years; lesion diameter 11 to 42 mm with an average of 22.9 ± 6.8 mm) were examined by both CECT and CEUS (CECT and CEUS group) within one week.

This study was approved by the hospital ethics committee, and written informed consent forms were obtained from all patients and their families.

### 2.2. Inclusion and exclusion criteria

#### 2.2.1. Inclusion criteria

The inclusion criteria were 1) definitive postoperative pathological diagnosis with complete clinical data, including CEUS and CECT; 2) signed informed consent forms; 3) normal communication and expression abilities.

#### 2.2.2. Exclusion criteria

The exclusion criteria were 1) under 18 years old; 2) pregnant or lactating women; 3) severe hepatic or renal insufficiency; 4) recent acute myocardial infarction, cerebral infarction, and severe pulmonary hypertension; 5) allergy to contrast agents; 6) preoperative percutaneous transhepatic GB drainage; 7) postoperative pathological confirmation of GB sludge; 8) unclear CEUS images.

### 2.3. CEUS

#### 2.3.1. Equipment and contrast agents

TOSHIBA Aplio 400, TOSHIBA Aplio 500, AcusonSequoia-31, and Mindray Resona 8 color Doppler ultrasound diagnostic systems were used, all equipped with abdominal convex array probes (1.0 to 5.0 MHz), high frequency probes (7.5 to 12.0 MHz), and real-time CEUS imaging software (mechanical index ≤ 0.1). The contrast agent used was sulfur hexafluoride microbubbles (SonoVue, Bracco, Italy).

#### 2.3.2. Procedure

After fasting for 8 hours, patients were placed in a supine position or a left lateral decubitus position at angle of 45 - 90°. Conventional US was performed first. For patients with multiple lesions, the largest lesion visible on US was selected for examination. Location, size, extent, echogenicity, and color Doppler flow features of the lesion were recorded. The optimal view was selected and switched to dual-mode CEUS. The contrast agent (2.4 mL) was diluted with 5 mL of 0.9% normal saline, vigorously shaken, and injected as a bolus *via* the antecubital vein, followed by 5 mL saline flush. CEUS images were observed and recorded for 3 min after injection. A second injection was performed at least 20 min after the first injection if initial enhancement was missed or the target lesion was lost.

#### 2.3.3. Image analysis

Two sonographers (> 10 years' CEUS experience) blind to each other's findings and the final diagnosis, independently analyzed the images, focusing on the following features: 1) enhancement phase: arterial phase (10-30 s post-injection) and venous phase(31-180 s); 2) enhancement level as compared with normal liver parenchyma or GB wall at the same depth: none, hypo-, iso-, or hyper-enhancement; 3) vascular

enhancement morphology: regular or irregular during the arterial phase; 4) enhancement pattern: homogeneous or heterogeneous enhancement within the lesion during the arterial phase. 5) GB wall integrity: continuous (all layers intact) or discontinuous (layer interruption). 6) border with adjacent liver tissue: well-defined or ill-defined. Quantitative parameters were observed *via* time-intensity curves (TICs), including arrival time (AT), arrival time of liver parenchyma (LAT), time to peak enhancement (TTP), rise time (RT), and washout time (WT).

2.4. CECT

2.4.1. Equipment and contrast agent

Siemens Drive and Force whole-body spiral CT machines and non-ionic iodine contrast agent (Omnipaque™ 300) were used.

2.4.2. Procedure

After fasting for 4-6 h, the patient underwent a non-contrast liver scan in a supine position. Contrast (1.5 mL/kg) was injected *via* antecubital vein at 3.5 to 4 mL/s using an automatic pressure injector. The scan was triggered using bolus-tracking technology (cursor at T12 level aorta and threshold at 100 HU). Arterial phase (full liver, breath-hold at 18 s), portal phase (breath-hold at 50 s), and delayed phase (after 100 s) were acquired.

2.4.3. Image analysis

Images were recorded and post-processed using a secondary workstation (Syngo MMWP version 2008C, Siemens Healthcare). Two other experienced radiologists, blind to the final diagnosis, recorded and analyzed changes in tumor morphology, vascularity, enhancement patterns in the arterial and venous phases (homogeneous/heterogeneous, hyper-enhancement/iso-enhancement/hypo-enhancement), local extension, fat planes with surrounding structures, and necrotic lymph nodes.

2.5. Statistical analysis

Statistical analysis was performed using Stata 11.0 software. Continuous variables were presented as mean ± SD, and categorical variables were presented as counts (n) and percentages (%). Histopathological findings served as the gold standard. For the entire cohort, the $\chi^2$ test was used to compare the imaging features of benign and malignant lesions between CEUS and CECT, as well as the diagnostic indices (sensitivity, specificity, accuracy, positive predictive value (PPV), negative predictive value (NPV)) of the two modalities. For the paired subgroup (52 patients in the CEUS and CECT groups), the paired $\chi^2$ test was used to compare the diagnostic efficacy of CEUS and CECT. The significance level was set at $\alpha = 0.05$, and $P < 0.05$ was considered statistically significant.

## 3. Results

3.1. Histopathological findings

All 151 patients underwent surgical resection with confirmed histopathological results (Table 1). In the CEUS group ($n$ = 126), 74 (58.7%) were histopathologically diagnosed as malignant and 52 (41.3%) as benign. In the CECT group ($n$ = 77), 40 (51.9%) were histopathologically diagnosed as malignant and 37 (48.1%) as benign. In the CEUS and CECT group ($n$ = 52), 20 (38.5%) were histopathologically diagnosed as malignant (Figure 1) and 32 (61.5%) as benign (Figures 2 and 3). Among 17 adenomas according to WHO classification (*19*) in the CEUS and CECT group, 9 were papillary adenomas, including 6 with atypical hyperplasia and 4 with malignant transformation; 6 were tubular adenomas, including 4 with atypical hyperplasia and 2 with malignant transformation; 2 were tubulopapillary adenomas, both with atypical hyperplasia and 1 with malignant transformation. All 7 adenomas with malignant transformation were classified into the malignant adenocarcinoma group, and the remaining 10

**Table 1. Histopathological findings of 151 GB lesions**

| Histopathological type | CECT | CEUS | BOTH |
|---|---|---|---|
| Malignant | | | |
| Adenocarcinoma | 31 (40.3) | 59 (46.8) | 17 (32.7) |
| Squamous cell carcinoma | 5 (6.5) | 8 (6.3) | 1 (1.9) |
| Adenosquamous carcinoma | 3 (3.9) | 5 (4.0) | 1 (1.9) |
| Papillary carcinoma | 1 (1.3) | 2 (1.6) | 1 (1.9) |
| ALL | 40 (51.9) | 74 (58.7) | 20 (38.5) |
| Benign | | | |
| Xanthogranulomatous cholecystitis | 7 (9.1) | 10 (7.9) | 6 (11.5) |
| Gallbladder adenomyomatosis | 6 (7.8) | 7 (5.6) | 5 (9.6) |
| Chronic cholecystitis | 7 (9.1) | 5 (4.0) | 4 (7.7) |
| Adenoma | 10 (13.0) | 17 (13.5) | 10 (19.2) |
| Cholesterol polyp | 7 (9.1) | 13 (10.3) | 7 (13.5) |
| ALL | 37 (48.1) | 52 (41.3) | 32 (61.5) |
| Total | 77 (100) | 126 (100) | 52 (100) |

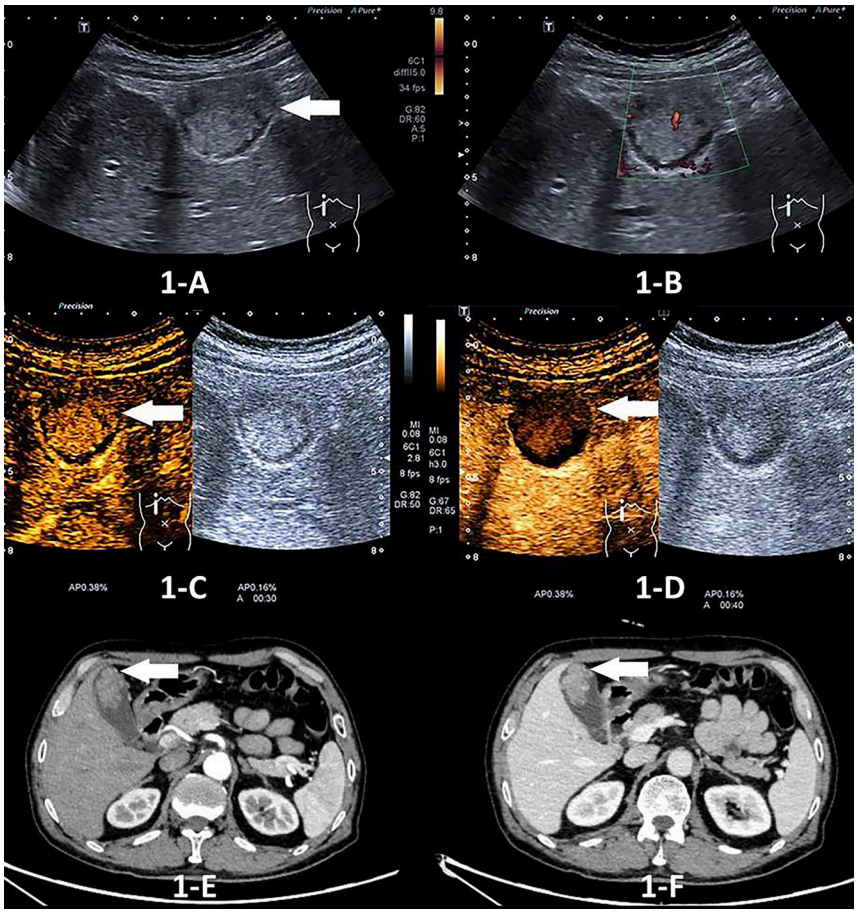


**Figure 1. A 67-year-old man with a 26.3 × 16.6 mm GBC was diagnosed using CEUS and CECT. (A-B)**: A mildly hyperechoic lesion located in the fundus of GB (arrow) and power Doppler showed a few strip-like blood flow signals on conventional ultrasound. **(C-D)**: The tumor was of heterogenous hyper-enhancement in the arterial phase (arrow) and washout at 40 s in the late phase (arrow) on CEUS. **(E-F)**: The lesion was obviously enhanced in the arterial phase (arrow) and hypo-enhancement in the venous phase as compared to liver (arrow) on CECT.

into the benign adenoma group.

3.2. Comparison of US, CEUS and CECT imaging features in 52 cases of benign and malignant GB lesions

On US, color Doppler showed that intralesional vascularity was significantly associated with malignant lesions ($P = 0.012$). On CEUS, irregular tumoral enhancement ($P < 0.001$), heterogeneous internal enhancement ($P = 0.002$), GB wall destruction ($P < 0.001$), and ill-defined border with adjacent liver tissue ($P < 0.001$) were significantly associated with malignant lesions. On CECT, arterial hyper-enhancement ($P < 0.001$), heterogeneous internal enhancement ($P < 0.001$), GB wall destruction ($P < 0.001$), ill-defined border with adjacent liver tissue ($P < 0.001$), necrotic lymph nodes ($P < 0.001$), and distant metastases ($P < 0.001$) were significantly associated with malignant lesions. Comparison of CEUS and CECT imaging features between benign and malignant GB lesions is presented in Table 2.

3.3. Quantitative analysis of CEUS TICs for GB lesion assessment

No significant differences were observed between benign and malignant lesions in AT, LAT, RT, or TTP (Table 3). Malignant lesions exhibited significantly earlier washout than benign lesions (WT: 38.1 ± 13.7 seconds *vs.* 71.4 ± 26.9 seconds, $P < 0.001$). Receiver operating characteristic (ROC) curve analysis determined a WT cutoff value of 46.3 seconds for diagnosing malignant lesions, with a sensitivity of 88.2%, specificity of 84.5%, and area under the curve (AUC) of 0.900.

3.4. Comparison of diagnostic efficiency of CEUS and CECT for GBC

CEUS diagnosed 77 malignant lesions, with 66 accurate diagnoses and 11 misdiagnoses (3 chronic cholecystitis, 3 xanthogranulomatous cholecystitis, 5 adenomas). It diagnosed 49 benign lesions, with 41 accurate diagnoses and 8 misdiagnoses (5 adenocarcinomas, 2 squamous cell carcinomas, 1 adenosquamous carcinoma). CECT diagnosed 45 malignant lesions, with 36 accurate diagnoses and 9 misdiagnoses (3 cholesterol polyps, 1 xanthogranulomatous cholecystitis, 3 adenomas, 2 chronic cholecystitis).

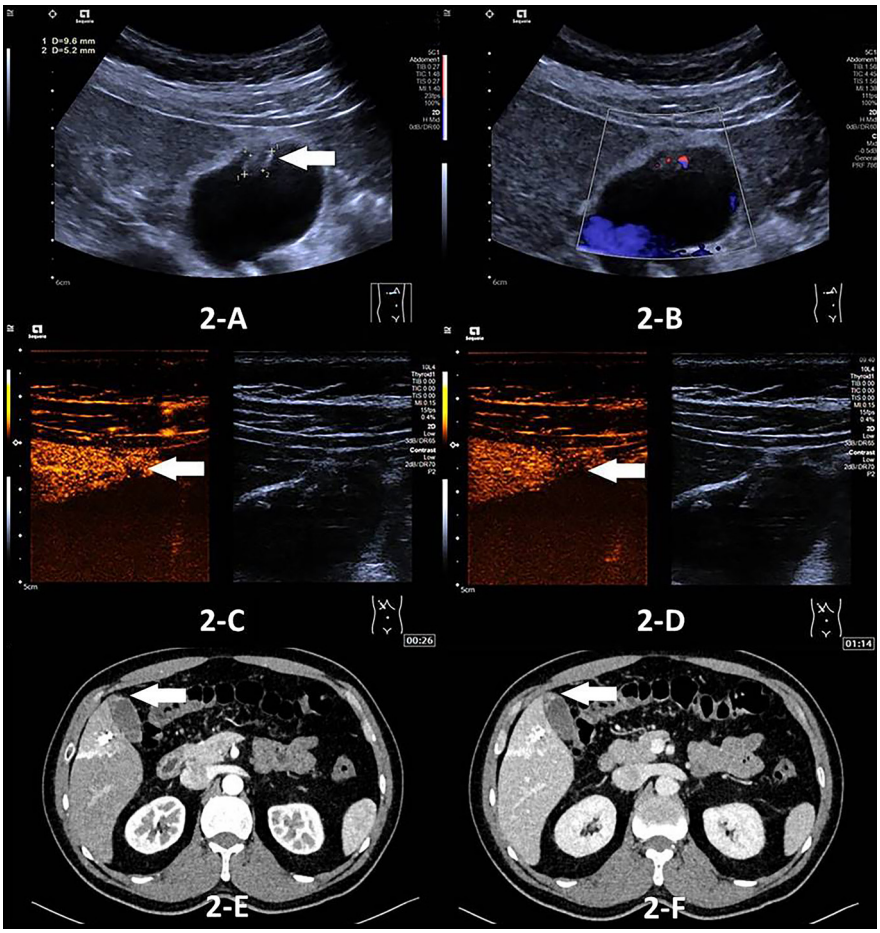


**Figure 2. A 44-year-old man with a 9.6 × 5.2 mm xanthogranulomatous cholecystitis diagnosed using CEUS and CECT. (A-B)**: A mildly hyperechoic lesion fundus of GB (arrow) and Color Doppler blood flow imaging (CDFI) showed a few strip-like flow signals on conventional ultrasound. **(C-D)**: No obvious contrast agent filling was observed throughout, and a small amount of GB wall destruction was visible (arrows) on CEUS. **(E-F)**: The lesion showed homogenous iso-enhancement, similar to the liver (arrow) in the arterial phase and prolonged enhancement (arrow) in the venous phase on CECT.

It diagnosed 32 benign lesions, with 26 accurate diagnoses and 6 misdiagnoses (4 adenocarcinomas, 1 papillary carcinoma, 1 adenosquamous carcinoma). Based on the histopathological gold standard, the diagnostic efficacy of CEUS and CECT was further compared in both the entire cohort and the paired subgroup. The sensitivity (89.2% *vs.* 85.7%), specificity (78.8% *vs.* 74.3%), accuracy (84.9% *vs.* 80.5%), PPV (85.7% *vs.* 80.0%), and NPV (83.7% *vs.* 81.2%) between CEUS and CECT in diagnosing benign and malignant GB lesions were no statistically significant differences ($P > 0.05$ for all) (Table 4). In the paired subgroup of 52 patients of the CEUS and CECT group, CEUS demonstrated a sensitivity of 65.0% (13/20), specificity of 62.5% (20/32), accuracy of 63.5% (33/52), PPV of 40.6% (13/32), and NPV of 51.3% (20/39); whereas CECT showed a sensitivity of 80.0% (16/20), specificity of 80.0% (24/32), accuracy of 76.9% (40/52), PPV of 50.0% (16/32), and NPV of 66.7% (24/36). No statistically significant differences were detected between the two modalities in the paired subgroup (all $P > 0.05$).

## 4. Discussion

Gallbladder polypoid lesions are categorized into neoplastic and non-neoplastic categories. Neoplastic lesions include gallbladder cancer and gallbladder adenoma, while non-neoplastic lesions include cholesterol polyps, inflammatory polyps, and gallbladder adenomyomatosis. GBC is a malignant tumor that seriously threatens human health, with adenocarcinoma being the most common pathological type. Other types include squamous cell carcinoma, adenosquamous carcinoma, neuroendocrine carcinoma, clear cell carcinoma, and signet ring cell carcinoma (*20*). Early-stage GBC lacks obvious clinical symptoms, with a detection rate of only about 23% (*21*). Most GBC patients are diagnosed at advanced stages, losing surgical opportunities (*22*). In recent years, its incidence and mortality have risen significantly (*23,24*), making early diagnosis and treatment crucial. CEUS and CECT are primary methods for diagnosing gallbladder lesions.

CECT offers high clarity and spatial resolution, providing information on tumor location and size, liver

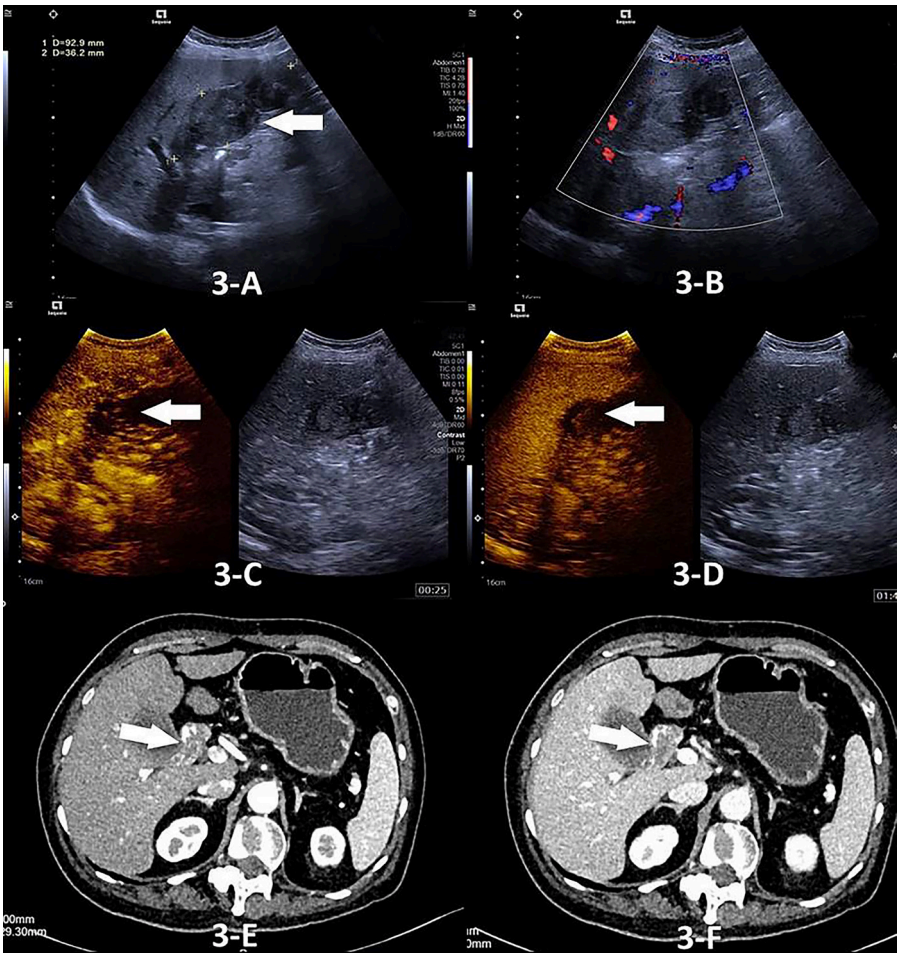


**Figure 3. A 68-year-old woman with a 23.5 × 21.4 mm polypoid lesion of GB was diagnosed using CEUS and CECT. (A-B)**: The GB was filled with heterogeneous hypoechoic and a few stones while CDFI showed no blood flow signals. **(C-D)**: The lesion was heterogeneous hyper-enhancement simultaneously with the GB wall in the arterial phase (arrow) and hypo-enhancement in late phase (arrow) on CEUS. **(E-F)**: The lesion shows heterogeneous hyper-enhancement with calcification at the margin in the arterial phase (arrow) and hyper-enhancement in late phase (arrow).

**Table 2. US, CEUS, and CECT features of 52 GB lesions**

| | Benign ($n$ = 32) | Malignant ($n$ = 20) | $P$ value |
|---|---|---|---|
| Gender (F/M) | 12/20 | 9/11 | 0.592 |
| Age (years)[a] | 53.6 ± 11.2 (32-82) | 56.8 ± 15.9 (41-87) | 0.614 |
| **US** | | | |
| Size | 23.9 ± 9.2 (23-41) | 33.7 ± 11.8 (29-46) | 0.061 |
| Cholelithiasis | 11 (34.4%) | 7 (35.0%) | 0.963 |
| Echogenicity hyper/iso/hypo/mixed | 12/8/6/6 | 2/5/5/8 | 0.135 |
| Positive intralesional vascularity on color doppler | 11 (34.4%) | 14 (70.0%) | 0.012* |
| **CEUS** | | | |
| Arterial phase enhancement hyper/iso (hypo) | 25/7 | 16/4 | 0.872 |
| Enhancement pattern in the arterial phase: regular and irregular | 29/3 | 2/18 | < 0.001* |
| the homogeneity of enhancement: homogenous/heterogeneous | 25/7 | 7/13 | 0.002* |
| Enhancement in the venous phase: hyper (iso) / hypo | 6/26 | 5/15 | 0.591 |
| Disruption of GB wall | 6 (18.8%) | 19 (95.0%) | < 0.001* |
| Border with surrounding liver tissue: clear/unclear | 28/4 | 6/14 | < 0.001* |
| **CECT** | | | |
| Cholelithiasis | 7 (21.9%) | 5 (25.0%) | 0.795 |
| Hyper-enhancement in the arterial phase | 9 (28.1%) | 17 (85.0%) | < 0.001* |
| Heterogeneous enhancement in the arterial phase | 5 (15.6%) | 14 (70.0%) | < 0.001* |
| Disruption of GB wall | 6 (18.9%) | 18 (90.0%) | < 0.001* |
| Border with surrounding liver tissue: clear/unclear | 4/28 | 14/6 | < 0.001* |
| hypo-enhancement in the venous phase | 7 (21.9%) | 9 (45.0%) | 0.079 |
| Necrotic nodes | 0 | 8 (40%) | < 0.001* |
| distant metastasis | 0 | 4 (20%) | < 0.001* |

**Table 3. Quantitative time intensity curve analysis of CEUS examinations**

| Contrast enhancement phase | Benign ($n$ = 32) / s | Malignant ($n$ = 20) / s | $P$ value |
|---|---|---|---|
| AT (s) [a] | 17.6 ± 5.7 (6-26) | 15.9 ± 5.1 (3-23) | 0.595 |
| LAT (s) [a] | 20.9 ± 7.1 (8-39) | 15.7 ± 5.2 (5-26) | 0.123 |
| RT(s) [a] | 6.7 ± 1.9 (7-13) | 5.3 ± 1.7 (4-11) | 0.372 |
| TTP(s) [a] | 25.1 ± 6.3 (14-37) | 21.1 ± 6.7 (9-31) | 0.069 |
| WT(s) [a] | 71.4 ± 26.9 (43-139) | 38.1 ± 13.7 (21-107) | < 0.001* |

**Table 4. Comparison of the accuracy between CEUS and CECT in the diagnosis of GBC**

| Methods | Sensitivity | Specificity | Accuracy | PPV | NPV |
|---|---|---|---|---|---|
| CECT | 36/42 (85.7%) | 26/35 (74.3%) | 62/77 (80.5%) | 36/45 (80.0%) | 26/32 (81.2%) |
| CEUS | 66/74 (89.2%) | 41/52 (78.8%) | 107/126 (84.9%) | 66/77 (85.7%) | 41/49 (83.7%) |
| $P$ value | 0.581 | 0.620 | 0.415 | 0.411 | 0.778 |

invasion, depth of liver invasion, metastasis, vascular invasion, and involvement of regional lymph nodes and distant organs. It quantifies lesion density by CT values to distinguish the components, *e.g.* fat, water, or calcification, aiding lesion characterization.

SonoVue, a second-generation ultrasound contrast agent, consists of sulfur hexafluoride microbubbles with a phospholipid shell that demonstrates favorable flexibility and stability. The microbubbles resonate at low acoustic pressure and persist long in blood. CEUS, through contrast imaging, overcomes limitations of conventional grayscale ultrasound and color Doppler ultrasound in imaging accuracy. It not only clearly reflects the hemodynamic changes at the lesion site but also provides sufficient time to observe the dynamic changes of tumor enhancement during contrast imaging, significantly aiding tumor differentiation.

In this study, malignancies diagnosed by both CECT and CEUS are predominantly adenocarcinomas (31/40 or 77.5% *vs.* 59/74 or 79.7%), followed by squamous cell carcinomas, adenosquamous carcinomas, and papillary carcinomas, which is consistent with the study by Moeini A *et al.* (*20*). Gallbladder adenomas is a common benign GB tumor, with an incidence of 0.2% to 0.5% (*25*) and a canceration rate of about 30% (*26*). In this study, 7 adenoma cases showed precancerous lesions, with a canceration rate of 41.2%, slightly higher than that reported in the literature (*26*).

Conventional ultrasound in this study revealed no significant differences between benign and malignant groups in lesion size, internal echogenicity, and gallstones. However, color Doppler ultrasound showed significantly higher intralesional vascularity in malignancies than in benign masses, aligning with the results of Hirooka Y *et al.* (*27*). Color Doppler blood flow detection is easily affected by lesion size, intralesional blood flow velocity, and instrument sensitivity. In addition, conventional ultrasound inadequately assesses GB wall integrity and liver involvement.

Previous studies comparing the diagnostic efficacy of US and CEUS for gallbladder diseases found superior sensitivity and specificity of CEUS over US but lacked detailed analysis of CEUS features of gallbladder malignant lesions and quantitative analysis using time-intensity curves (*11,28*). Another study involving 1,044 patients with gallbladder space-occupying lesions reported a sensitivity of 81%, a specificity of 87%, a diagnostic odds ratio of 58.84, and an AUC of 0.93 of CEUS in differentiating gallbladder lesion (*18*). Similarly, this study did not provide specific CEUS features. Bo X *et al.* compared the diagnostic accuracy of various imaging modalities in differentiating gallbladder cancer from xanthogranulomatous cholecystitis and found higher CEUS sensitivity and specificity than CECT (*29*), but did not compare CEUS and CECT for other lesions. In a meta-analysis of 25 studies involving 2,469 patients with focal gallbladder lesions, Zhang L *et al.* found that CEUS and CECT had comparable diagnostic efficacy but omitted feature analysis (*30*).

This current study aimed to investigate the value of CEUS and time-intensity curves in differentiating benign and malignant gallbladder lesions and to compare the diagnostic efficacy of CEUS and CECT. Irregular enhancement (CEUS), heterogeneous enhancement (CEUS), GB wall disruption (CEUS or CECT), ill-defined border with adjacent liver tissue (CEUS or CECT), WT (CEUS), and arterial hyper-enhancement (CECT) were found to be significantly associated with malignancies, suggesting that CEUS has an important role to play in describing abnormal gallbladder features detected by imaging examinations.

Unlike the liver, the GB has single-artery blood supply (cystic artery), resulting in stronger wall enhancement than the liver parenchyma. Arterial hyper-enhancement was observed in 16 GBC cases (16/20, 75.0%) due to GBC growth, invasion, and metastasis as a result of high-density neovascularization. However, 25 (25/32, 78.1%) benign lesions also exhibited arterial hyper-enhancement, probably attributable to inflammation-induced angiogenesis, with no statistical

differences between the benign and malignant groups. Xie XH *et al.* (*16*) studied GBC 33 patients and 47 patients with benign gallbladder diseases and concluded that arterial hyper-enhancement could not differentiate benign and malignant gallbladder space-occupying lesions, which is consistent with our findings. Inoue T *et al.* (*31*) and Numata K *et al.* (32) also noted limited diagnostic value of CEUS vascularity for gallbladder diseases using a coded phase-inversion harmonic US and Levovist.

Tumor neovascularization is of great significance for the occurrence and development of malignancies, and vascular morphology provides diagnostic basis for CEUS. Four main vascular type have been identified in gallbladder lesions, *i.e.* punctate, linear, branched, and irregular. In our cohort, 90.0% (18/20) malignancies presented irregular patterns against 90.6% (29/32) regular patterns (punctate, linear, and branched) in benign lesions, without statistically significant difference ($P < 0.05$). This observation is attributable to rich large and irregular neovessels (twisted and deformed with dense clusters) in malignancies and a tendency to form a large number of arteriovenous shunts, thus often an irregular pattern on CEUS. In contrast, neovascularization in benign gallbladder lesions is slow, with a single flow pattern and fewer branches, which is closer to normal tissue (*33*).

Heterogeneous perfusion was observed in 65.0% (13/20) malignancies, significantly higher than 21.9% (7/32) in benign lesions ($P < 0.05$), consistent with previous studies (*26,34*). The reason lies the disorganized neovascularization in malignant tumors, which can cause uneven vascular distribution. In addition, neovessels within malignant tumors cannot supply sufficient nutrients required for the rapid growth. Consequently, ischemic necrosis occurs within the tumor, manifesting asheterogeneous enhancement on CEUS.

Most benign gallbladder lesions exhibit homogeneous internal echogenicity. However, in some patients with cholecystitis and gallbladder adenomyomatosis, due to acute and chronic inflammation or the formation of Rokitansky-Aschoff sinuses within the gallbladder wall at the lesion area, hypo-enhancement or non-enhanced areas appear, showing heterogeneous perfusion on CEUS.

Gallbladder cancer originates from atypical mucosal hyperplasia and gradually progresses to carcinoma in situ, invasive carcinoma, surrounding tissue invasion, and distant metastasis. Therefore, evaluating the structural integrity of the gallbladder wall is of great significance for the diagnosing GBC (*33*). In this study, 19 cases (19/20, 95.0%) of gallbladder cancer exhibited varying degrees of gallbladder wall destruction, among which 14 showed ill-defined borders with adjacent liver tissue. Kong WT *et al.* (*35*) found that the blurred boundary between the gallbladder wall and the liver was an independent predictor of malignancy in 49 gallbladder lesions. Xie XH *et al.* (*16*) found that gallbladder wall destruction highly predicted malignancy, with a sensitivity of 84.8% and a specificity of 100%. Chen LD *et al.* (*17*) claimed that an interrupted inner layer was an independent predictor of malignancy. US is barely satisfactory in evaluating the thickness, continuity, and internal echogenicity of the gallbladder wall, whereas CEUS can not only clearly display the mucosal and serosal layers of the gallbladder wall but also perform real-time scanning and acquire data (*17,36*). Therefore, CEUS is more effective for diagnosing benign and malignant gallbladder lesions.

Hypo-enhancement in the delayed phase is an important CEUS feature of hepatic malignancies, but it is not applicable to gallbladder lesions because all gallbladder cancers and most benign gallbladder diseases exhibit hypo-enhancement in the delayed phase, as demonstrated in this study. The reason for this phenomenon may be related to the fact that gallbladder blood supply is solely provided by branches of the hepatic artery. Due to the absence of portal vein supply, the persistence of contrast agent in the venous phase shortens, thus potentially being misinterpreted as washout, especially for small lesions. On the other hand, we consider contrast agent WT to be a useful feature for differentiating benign and malignant gallbladder lesions. In this study, with a WT cutoff value of 46.3 s, its sensitivity for diagnosing malignant lesions was 89.4%, specificity was 86.1%, and AUC was 0.900. However, opinions vary regarding the optimal cutoff value for contrast agent washout. Xie XH *et al.* (*16*) proposed 35 s as the critical cutoff value for WT, with a sensitivity of 90.9% and a specificity of 87.2% in malignancy diagnosis. Serra C *et al.* (*37*) and Wang W *et al.* (*38*) suggested 60 s as the optimal cut-off value for defining malignancy with higher diagnostic accuracy.

In our study, 4 adenoma cases s with canceration were misdiagnosed as adenomas due to the small size of the lesions (all smaller than 2 cm) and the presence of benign lesion features on CEUS. Regarding CEUS manifestations of adenoma canceration, some researchers (*39*) believe that gallbladder adenomas after canceration demonstrate "slow enhancement and rapid washout", whereas Hattori M *et al.* (*40*) studied 60 gallbladder space-occupying lesions and concluded that the CEUS manifestations of adenoma canceration are identical to those of gallbladder cancer, both showing "rapid enhancement and rapid washout". However, only two gallbladder adenoma lesions were included in their study, thus the results are not generalizable. The reason for discrepancies in CEUS manifestations of cancerated adenomas may be ascribed to differences in patient populations, such as clinical profiles, disease stages, and age. Thus, accurate diagnosis of early-stage GBC remains a challenge for ultrasound.

In the benign group of this study, four benign cases

were misdiagnosed as malignant tumors due to the displayed interruption of GB wall integrity. Among them, 2 cases had cholecystitis with perforation, and liver inflammatory lesions secondary to perforation were misinterpreted as tumor invasion on CEUS. The other two cases were of xanthogranulomatous cholecystitis and also exhibited incomplete GB walls, possibly due to the release of phospholipase A from the GB mucosal epithelium stimulated by inflammation or bile stasis, which hydrolyzes lecithin in bile into lysophosphatidylcholine. The latter further destroys the integrity of the mucosal epithelial cells and causes irregular morphology of the mucosal layer. The authors consider that ill-defined borders between the gallbladder wall and liver tissue, along with significant wall thickening and loss of normal structure, can be regarded as malignant features, whereas mere continuity interruption requires consideration of possibile benign lesions.

This study included three adenomas misdiagnosed as malignant due to short contrast agent WT. This indicates that using rapid washout as a predictor for malignancy may cause false positives in lesions. Therefore, the role of the optimal cutoff value of WT in differentiating benign and malignant gallbladder lesions still warrants further evaluation.

This study used pathological results as the gold standard, finding that CEUS outperformed CECT in diagnosing gallbladder cancer in the respects of sensitivity (89.2% *vs.* 85.7%), specificity (78.8% *vs.* 74.3%), accuracy (84.9% *vs.* 80.5%), PPV (85.7% *vs.* 80.0%), and NPV (83.7% *vs.* 81.2%), but without statistical significance ($P > 0.05$). CECT showed poor accuracy in diagnosing benign gallbladder lesions. In other words, it more readily tended to misdiagnose them as malignant. The reason might lie in CECT's limitation to cross-sectional scanning. For some benign lesions, the pedicle could not be observed, only displaying broad-based soft tissue shadows protruding into the gallbladder lumen with significant arterial enhancement and thus easily misdiagnosed as malignant lesions. In addition, CECT could only select scanning times empirically and could not visualize real-time enhancement process. This makes it highly susceptible to individual patient differences and operator experience, preventing accurate observation of the enhancement patterns at peak enhancement, particularly for small gallbladder lesions where CT scanning poses difficulties in summarize the enhancement characteristics. In this cohort, 9 benign lesions (3 cholesterol polyps, 1 xanthogranulomatous cholecystitis, 3 adenomas, and 2 chronic cholecystitis) were misdiagnosed as malignant by CECT. However, compared with CEUS, CECT had certain advantages in detecting retroperitoneal lymph node metastasis, distant metastasis, and intrahepatic metastasis within ultrasound blind zones (*4*). Among the 2 CEUS-misdiagnosed gallbladder cancer cases, CECT diagnosed 1 case with gallbladder cancer with necrotic retroperitoneal lymph nodes and 1 case with omental infiltration before surgery. Thus, in displaying gallbladder lesions, CECT offers advantages over CEUS in evaluating the degree and extent of lesion invasion of surrounding tissues and occurrence of lymph node metastasis.

Some limitations are mentionable. This study did not include thick-walled GB lesions which might lead to statistical bias. Second, the number of cases diagnosed by both CEUS and CECT is small; therefore, the diagnostic value of the former should be validated in subsequent studies with larger patient cohorts. Finally, our study was retrospective in nature. In future studies, a prospective, paired design should be employed, where all enrolled patients undergo both CEUS and CECT examinations simultaneously. This will allow for direct, one-to-one comparison using pathology as the gold standard, maximizing statistical power and yielding more reliable conclusions.

CEUS facilitates differentiation between benign and malignant GB lesions and holds high diagnostic value, warranting clinical promotion and application. In our present study, the diagnostic efficacy of CEUS was found comparable to that of CECT. CEUS can serve as an alternative to CECT in patients with iodine contrast anaphylaxis or renal insufficiency. The two modalities can complement each other and provide more valuable information for the differential diagnosis of GB lesions, thereby improving diagnostic accuracy.

*Funding*: This work was supported by a grant from Shanghai Municipal Health Commission (grant No. 202340140 to ZY Qiu), and the National Natural Science Foundation of China (grant No. 82374243 to L Wang).

*Conflict of Interest*: The authors have no conflicts of interest to disclose.

## References

1. Lazcano-Ponce EC, Miquel JF, Muñoz N, Herrero R, Ferrecio C, Wistuba II, Alonso de Ruiz P, Aristi Urista G, Nervi F. Epidemiology and molecular pathology of gallbladder cancer. CA Cancer J Clin. 2001; 51:349-364.
2. Sharma A, Sharma KL, Gupta A, Yadav A, Kumar A. Gallbladder cancer epidemiology, pathogenesis and molecular genetics: Recent update. World J Gastroenterol. 2017; 23:3978-3998.
3. Mao W, Deng F, Wang D, Gao L, Shi X. Treatment of advanced gallbladder cancer: A SEER-based study. Cancer Med. 2020; 9:141-150.
4. Hundal R, Shaffer EA. Gallbladder cancer: epidemiology and outcome. Clin Epidemiol. 2014; 6:99-109.
5. Yuan B, Zhao X, Wang X, Liu E, Liu C, Zong Y, Jiang Y, Hou M, Chen Y, Chen L, Zhang Y, Wang H, Fu J. Patient-derived organoids for personalized gallbladder cancer modelling and drug screening. Clin Transl Med. 2022; 12:e678.

6. Nie C, Yang T, Liu L, Hong F. Trend analysis and risk of gallbladder cancer mortality in China, 2013-2019. Public Health. 2022; 203:31-35.
7. Torre LA, Siegel RL, Islami F, Bray F, Jemal A. Worldwide Burden of and Trends in Mortality From Gallbladder and Other Biliary Tract Cancers. Clin Gastroenterol Hepatol. 2018; 16:427-437.
8. Feo CF, Ginesu GC, Fancellu A, Perra T, Ninniri C, Deiana G, Scanu AM, Porcu A. Current management of incidental gallbladder cancer: A review. Int J Surg. 2022; 98:106234.
9. Wernberg JA, Lucarelli DD. Gallbladder cancer. Surg Clin North Am. 2014; 94:343-360.
10. Gore RM, Thakrar KH, Newmark GM, Mehta UK, Berlin JW. Gallbladder imaging. Gastroenterol Clin North Am. 2010; 39:265-ix.
11. Zhang HP, Bai M, Gu JY, He YQ, Qiao XH, Du LF. Value of contrast-enhanced ultrasound in the differential diagnosis of gallbladder lesion. World J Gastroenterol. 2018; 24:744-751.
12. Liang X, Jing X. Meta-analysis of contrast-enhanced ultrasound and contrast-enhanced harmonic endoscopic ultrasound for the diagnosis of gallbladder malignancy. BMC Med Inform Decis Mak. 2020; 20:235.
13. Fang L, Bai K, Chen Y, Zhan J, Zhang Y, Qiu ZY, Chen L, Wang L. A comparative study of contrast-enhanced ultrasound and contrast-enhanced CT for the detection and characterization of renal masses. Biosci Trends. 2021; 15:24-32.
14. Fang L, Zhu Z, Huang BJ, Ding H, Mao F, Li C, Zeng M, Zhou J, Wang L, Wang W, Chen Y. A comparative study of contrast enhanced ultrasound and contrast enhanced magnetic resonance imaging for the detection and characterization of hepatic hemangiomas. Biosci Trends. 2015; 9:104-110.
15. Xu JM, Guo LH, Xu HX, Zheng SG, Liu LN, Sun LP, Lu MD, Wang WP, Hu B, Yan K, Hong D, Tang SS, Qian LX, Luo BM. Differential diagnosis of gallbladder wall thickening: the usefulness of contrast-enhanced ultrasound. Ultrasound Med Biol. 2014; 40:2794-2804.
16. Xie XH, Xu HX, Xie XY, Lu MD, Kuang M, Xu ZF, Liu GJ, Wang Z, Liang JY, Chen LD, Lin MX. Differential diagnosis between benign and malignant gallbladder diseases with real-time contrast-enhanced ultrasound. Eur Radiol. 2010; 20:239-248.
17. Chen LD, Huang Y, Xie XH, Chen W, Shan QY, Xu M, Liu JY, Nie ZQ, Xie XY, Lu MD, Shen SL, Wang W. Diagnostic nomogram for gallbladder wall thickening mimicking malignancy: using contrast-enhanced ultrasonography or multi-detector computed tomography. Abdom Radiol (NY). 2017; 42:2436-2446.
18. Cheng Y, Wang M, Ma B, Ma X. Potential role of contrast-enhanced ultrasound for the differentiation of malignant and benign gallbladder lesions in East Asia: A meta-analysis and systematic review. Medicine (Baltimore). 2018; 97:e11808.
19. Wu MC. Liver malignant diseases. In: Huang Jiasi Surgery(Wu JP, Qiu FZ, eds.). People's Medical Publishing House, Beijing, China, 2002; pp. 1223.
20. Moeini A, Haber PK, Sia D. Cell of origin in biliary tract cancers and clinical implications. JHEP Rep. 2021; 3:100226.
21. Pradhan S, Shukla VK, Agrawal S, Dixit VK, Sharma OP. Sonographic and colour doppler morphology in carcinoma gallbladder. Indian J Cancer. 2002; 39:143-148.
22. Li J, Wu XR, Yu TZ. Comparative analysis of contrast-enhanced ultrasound and contrast-enhanced CT in differential diagnosis of benign and malignant space-occupying lesions of gallbladder. Int J Biomed Eng. 2018; 41:261-264+270.
23. Sung H, Ferlay J, Siegel RL, Laversanne M, Soerjomataram I, Jemal A, Bray F. Global Cancer Statistics 2020: GLOBOCAN Estimates of Incidence and Mortality Worldwide for 36 Cancers in 185 Countries. CA Cancer J Clin. 2021; 71:209-249.
24. Xia C, Dong X, Li H, Cao M, Sun D, He S, Yang F, Yan X, Zhang S, Li N, Chen W. Cancer statistics in China and United States, 2022: profiles, trends, and determinants. Chin Med J (Engl). 2022; 135:584-590.
25. Pang L, Zhang Y, Wang Y, Kong J. Pathogenesis of gallbladder adenomyomatosis and its relationship with early-stage gallbladder carcinoma: an overview. Braz J Med Biol Res. 2018; 51:e7411.
26. Sun LP, Guo LH, Xu HX, Liu LN, Xu JM, Zhang YF, Liu C, Bo XW, Xu XH. Value of contrast-enhanced ultrasound in the differential diagnosis between gallbladder adenoma and gallbladder adenoma canceration. Int J Clin Exp Med. 2015; 8:1115-1121.
27. Hirooka Y, Naitoh Y, Goto H, Furukawa T, Ito A, Hayakawa T. Differential diagnosis of gall-bladder masses using colour Doppler ultrasonography. J Gastroenterol Hepatol. 1996; 11:840-846.
28. Xing RW, Mu YH, Li WJ, Li B, Nie HQ, Yin P. Comparative analysis of contrast-enhanced ultrasound and enhanced CT in diagnosis of polypoid lesions of gallbladder. Gan Dan Yi Wai Ke Za Zhi. 2019; 6:356-359. (in Chinese)
29. Bo X, Chen E, Wang J, Nan L, Xin Y, Wang C, Lu Q, Rao S, Pang L, Li M, Lu P, Zhang D, Liu H, Wang Y. Diagnostic accuracy of imaging modalities in differentiating xanthogranulomatous cholecystitis from gallbladder cancer. Ann Transl Med. 2019; 7:627.
30. Zhang L, Tang Y, Gong J, Li Y, Li C, Wen M. Meta-analysis of the diagnostic value of contrast-enhanced CT and contrast-enhanced ultrasound in focal gallbladder lesions. Lin Chuang Fang She Xue Za Zhi. 2018; 2:271-6. (in Chinese)
31. Inoue T, Kitano M, Kudo M, Sakamoto H, Kawasaki T, Yasuda C, Maekawa K. Diagnosis of gallbladder diseases by contrast-enhanced phase-inversion harmonic ultrasonography. Ultrasound Med Biol. 2007; 33:353-361.
32. Numata K, Oka H, Morimoto M, Sugimori K, Kunisaki R, Nihonmatsu H, Matsuo K, Nagano Y, Nozawa A, Tanaka K. Differential diagnosis of gallbladder diseases with contrast-enhanced harmonic gray scale ultrasonography. J Ultrasound Med. 2007; 26:763-774.
33. Fei X, Luo YK. Interpretation and image analysis of gallbladder ultrasonography guideline. Zhonghua Yi Xue Chao Sheng Za Zhi. 2018; 15:5-10. (in Chinese)
34. Miwa H, Numata K, Sugimori K, Sanga K, Hirotani A, Tezuka S, Goda Y, Irie K, Ishii T, Kaneko T, Tanaka K, Maeda S. Differential diagnosis of gallbladder polypoid lesions using contrast-enhanced ultrasound. Abdom Radiol (NY). 2019; 44:1367-1378.
35. Kong WT, Shen HY, Qiu YD, Han H, Wen BJ, Wu M. Application of contrast enhanced ultrasound in gallbladder lesion: is it helpful to improve the diagnostic capabilities? Med Ultrason. 2018; 20:420-426.
36. Tang S, Wang Y, Wang Y. Contrast-enhanced ultrasonography to diagnose gallbladder perforation. Am J

Emerg Med. 2013; 31:1240-1243.
37. Serra C, Felicani C, Mazzotta E, Gabusi V, Grasso V, De Cinque A, Giannitrapani L, Soresi M. CEUS in the differential diagnosis between biliary sludge, benign lesions and malignant lesions. J Ultrasound. 2018; 21:119-126.
38. Wang W, Fei Y, Wang F. Meta-analysis of contrast-enhanced ultrasonography for the detection of gallbladder carcinoma. Med Ultrason. 2016; 18:281-228.
39. Sun LP, Guo LH, Xu HX, Liu LN, Xu JM, Zhang YF, Liu C, Bo XW, Xu XH. Value of contrast-enhanced ultrasound in the differential diagnosis between gallbladder adenoma and gallbladder adenoma canceration. Int J Clin Exp Med. 2015; 8:1115-1121.
40. Hattori M, Inui K, Yoshino J, Miyoshi H, Okushima K, Nakamura Y, Naito T, Imaeda Y, Horibe Y, Hattori T, Nakazawa S. Usefulness of contrast-enhanced ultrasonography in the differential diagnosis of polypoid GB lesions. Nihon Shokakibyo Gakkai Zasshi. 2007; 104:790-798. (in Japanese)

Received September 2, 2025; Revised December 4, 2025; Accepted December 9, 2025.

[§]These authors contributed equally to this work.

**Address correspondence to:*
Lin Chen, Department of Ultrasonic Diagnosis, Huadong Hospital Affiliated to Fudan University, 221 West Yanan Road, Shanghai 200040, China.
E-mail: hdchenlin@fudan.edu.cn

Ling Wang, Department of Obstetrics, The First Affiliated Hospital, Guizhou University of Traditional Chinese Medicine, No. 71 Baoshan North Road, Guiyang 550001, China.
E-mail: dr.wangling@vip.163.com

Released online in J-STAGE as advance publication December 16, 2025.